FINITE ELEMENT ANALYSIS OF SUPERPLASTIC BEHAVIOR OF MMCS IN PRESENCE OF SOME MANUFACTURING DEFECTS

A. Barakati, A. Abedian
Department of Aerospace Engineering,
Sharif University of Technology, Tehran, Iran

OVERVIEW

An axisymmetric micromechanical finite element model has been developed to predict the superplastic behavior of whisker reinforced Metal Matrix Composites. It has been reported that internal stress superplasticity can be utilized to enhance the ductility of whisker-reinforced metal matrix composites that are normally brittle. In particular, in this study the superplasticity behavior of $Al2024/SiCw$ is investigated as a typical MMC and the results obtained from the FE modeling are compared with some available experimental data. Some manufacturing defects such as various debonding ratios of fiber and matrix interface and strain hardening due to the superplastic deformation of the matrix are considered to improve the results of the modeling. The achievements of this simulation are in a good agreement with the reported experimental tests and the proposed model can be hired to have a proper prediction of the superplastic behavior of metal matrix composites.

1. NOMENCLATURE

AR_f	Fiber aspect ratio
AR_u	Unit aspect ratio
$\Delta V/V$	Volume mismatch
$\Delta\varepsilon$	Strain per cycle
$\dot{\varepsilon}$	Strain rate [s^{-1}]
$\bar{\varepsilon}_p$	Average plastic strain
m	Strain-rate sensitivity exponent
n	Stress exponent
N	Number of cycles
σ	Flow stress [Pa]
σ°	Externally applied stress [Pa]
σ_i	Internal stress [Pa]
σ_Y	Yield stress [Pa]
τ	Period of applied loads [s]
V_f	Fiber volume fraction
ζ	Debonding parameter
CTE	Coefficient of Thermal Expansion
FEM	Finite Element Method
FSS	Fine Structure Superplasticity
ISS	Internal Stress Superplasticity
MMC	Metal Matrix Composite

2. INTRODUCTION

Discontinuously reinforced metal matrix composites have been successfully manufactured through powder metallurgy technology in the last decade. This kind of MMCs is attractive for many structural applications because of their high specific strength and modulus of elasticity. However, in general, these materials have relatively low room temperature ductility which means that to certain extent they are not easy to be shaped. Even at elevated temperatures, they normally show only limited tensile ductility [1]. Recently, a number of researchers [2-7] have reported that some discontinuously reinforced aluminum MMCs could behave superplastically when tested under the right conditions. The advantages of using superplastic forming are not only weight reduction, but also improvement of the stress concentration, cost, and time of manufacturing.

Superplasticity is a phenomenon that has been observed widely in several kinds of materials due to the possibility of promoting the stress flow, such as metals (including aluminum, magnesium, iron, titanium and nickel-based alloys), intermetallics (including iron, nickel, and titanium base), ceramics (including monoliths and composites) and laminates [8]. In fact, Superplasticity is the ability of a polycrystalline material to exhibit, in a generally isotropic manner, very high tensile elongations prior to failure [9]. Superplastic materials have this characteristic because they exhibit flow stresses, σ, which are highly sensitive to the rate of deformation, $\dot{\varepsilon}$. That is, they have a high strain-rate sensitivity exponent, m, in the Backoften's relation $\sigma = K\dot{\varepsilon}^m$, with values typically equal to 0.5 or greater. When the strain-rate-sensitivity exponent is equal to unity and the relationship between $\dot{\varepsilon}$ and σ happens to be linear, the material is said to exhibit Newtonian-viscous behavior. The material can then behave like many non-crystalline materials such as heated glass. In such occasions, in crystalline materials, elongations of up to several hundred percentages or higher could happen without any trace of irregular or sharp changes in the cross section. This is a

desirable goal to achieve in superplastic crystalline materials although it could be rarely observed.

Two main types of superplastic behavior have been distinguished: Microstructural or Fine Structural Superplasticity (FSS), and Internal Stress Superplasticity (ISS). Fine-structured (grained) superplastic materials have a strain rate sensitivity exponent equal to about 0.5 (in most cases), and deform principally by a grain-boundary sliding mechanism. The most common superplastically formed products are made from fined grained sheets. The principal method is by blow forming, gas pressure being applied on one side of the sheet, whereby the sheet plastically flows into a die of predetermined shape and complexity. The structural prerequisites for FSS materials are fine grain size, presence and strength of the second phase, size and distribution of second phase, mobility of grain boundaries and shape of grains.

On the other hand, the internal-stress superplastic materials are usually characterized by a strain-rate-sensitivity exponent of unity, i.e., they exhibit Newtonian-viscous behavior. Such superplastic materials generally deform by a slip deformation mechanism through a phase change under thermal cycling (as in $Ni-Fe$ alloys), or due to having different Coefficients of Thermal Expansion (CTEs) in different directions (as in Zinc and $\alpha-$Uranium), or possessing phases with different CTEs (as in MMCs, like Al/SiC composites) [5-7]. Actually internal stress superplasticity is classified into transformation superplasticity and CTE-mismatch superplasticity depending on the type of generation mechanism of the mismatch strain. The ISS regime, since the plasticity occurs by means of slip deformation mechanism and the strain rate sensitivity is close to one, the grain size and shape are not of great importance.

It has been shown that internal stress superplasticity can be utilized to enhance the ductility of whisker-reinforced metal matrix composites that are normally brittle. The basis of understanding the effect of internal stress on enhancing the ductility of metal matrix composites is as follows. During thermal cycling, internal stresses are developed at the interfaces between the metal matrix and the hard ceramic second phase. This is because the thermal expansion coefficient of the matrix is several times larger than that of the ceramic phase. These internal stresses will relax by plastic deformation in the metal matrix to the value of the local interfacial yield stress of the material. It is this remaining local yield stress, that we define as the internal stress, σ_i, which contributes to the low applied external stress, and results in macroscopic deformation along the direction of the applied stress [6]. At room temperature, CTE-mismatch strains generally produce microcracks or grain boundary fractures, and then, the toughness or ductility of the materials decreases. This is because the materials cannot immediately accommodate the generated CTE-mismatch strain. However, if the CTE-mismatch strain is immediately accommodated at high temperatures, quite different deformation behavior appears in the material. It is called CTE-mismatch superplasticity, which is one type of internal stress superplasticity.

For transformation superplasticity, Greenwood and Johnson [7] assumed an ideally plastic material and derived a linear equation between the strain per cycle $\Delta\varepsilon$ and the externally applied stress σ° as

(1) $$\Delta\varepsilon = \frac{5}{3}\frac{\Delta V}{V}\frac{\sigma^\circ}{\sigma_Y}$$

where $\Delta V/V$ is the volume mismatch between the two allotropic phases and σ_Y is the yield stress of the weaker phase.

Wu *et al.* [7] attempted to apply Greenwood and Johnson's model to CTE-mismatch superplasticity by replacing the term of transformation mismatch $\Delta V/V$ with the term of CTE-mismatch. However, since the geometry of each material is quite different from the other, it is not appropriate to apply Greenwood and Johnson's model to CTE-mismatch superplasticity. So they considered CTE-mismatch superplasticity from another point of view and assumed that the material deforms according to *n-th* power law and that half of the dislocations experience a stress which is increased by the internal stress $\left|\sigma^\circ+\sigma_i\right|$, and the other half experience a stress which is reduced by the internal stress $\left|\sigma^\circ-\sigma_i\right|$. If the applied stress is much lower than the internal stress $\sigma^\circ \ll \sigma_i$, the deformation is described by the linear creep equation:

(2) $$\dot{\varepsilon} = nB(\sigma_i)^{n-1}\sigma^\circ$$

where B and n are the coefficient and the stress exponent of isothermal power-law creep, respectively.

Two different practical approaches based on the kind of loading, i.e. isothermal and thermal cycling, are employed for imposing superplastic deformation by the ISS mechanism. For the former approach, which is more common in practice, the forming is performed in a constant temperature. In this method, the strain rate is relatively high. However, for the latter approach, which is so called thermal cycling superplasticity, the strain rate is low and in average

it falls in the range of $10^{-5}-10^{-4}s^{-1}$. Additionally, the thermally cycled composites are much weaker than the isothermally tested composites at low applied stresses. Also, the thermally cycled composites have strain rate sensitivity exponents of unity at low stresses. Note that in general, the thermal cycling approach creates higher elongations compared to the isothermal approach [7,9].

The thermal cycling approach along with an external tensile mechanical stress, which is considered to be small and constant, is employed for superplastic forming of metal matrix composites reinforced with ceramic whiskers. Note that these materials have found much interest in the aerospace industry due to their superior properties. The difference in CTEs of the fiber and matrix creates large interfacial internal stresses which depending on the characteristics of the applied thermal cycle they could increase to the values higher than the yield strength of the matrix causing plastic deformation in the composite. However, since in this approach a thermal cycling regime is applied, the plastic strain totally vanishes when the temperature is reversed in the next half cycle. Here, the applied small mechanical stress biases the stress field generated during the thermal cycle, causing a small permanent plastic strain, which with repeating the thermal cycle, it starts to accumulate [4,10]. This has been developed into a more soundly based quantitative predictive model using the Lavy-von Mises flow rules and has been further developed for other cases of the phenomenon [11], where more details could also be found in [12].

Keeping in mind the complication involved, to understand the deformation mechanisms and the interrelationship between the constituents of the composites in the event of superplastic behavior, it is necessary to analyze the problem carefully. However, as the experimental works are time consuming, costly, and very equipment dependent, therefore, analytical and numerical tools, which have not widely been considered, must be developed. Since the analytical studies involve with very complicated PDEs that require so many assumptions to become solvable, numerical methods such as the Finite Element Method (FEM) may ease the solution. However, very careful geometry and material modeling, as well as the meshing and employing nonlinear procedures are necessary. It should be mentioned that due to the complications involved, only a few FEM studies would be found in the literature [13-17].

In the most recent FEM papers [12,19], assuming a regular distribution for the whiskers, an axisymmetric micromechanical model has been used for modeling the behavior of Al/SiC_W composite under superplastic loading conditions. Although the study showed that the modeling is fundamentally acceptable, there is still a long way for generalizing the approach. For example, due to some differences that were detected between the experimental data and the calculated FEM results [18,19], the model seems to need some modifications.

In present study, the effects of fiber/matrix debonding are being investigated for $Al2024/20\%SiC_W$. Some ratios of fiber/matrix debonding including 12.5%, 25%, 37.5% and 50% have been applied to the model and the results are compared with the results of the perfect bond simulation and some available experimental data. The new proposed method of gathering results from the FE model is quite acceptable. Also, the probable necking phenomenon in larger applied mechanical loads is analyzed by considering the strain hardening property for the matrix.

3. FINITE ELEMENT SIMULATION

Considering all various aspects of geometry, material types, and loading profile will definitely result in more precise and reliable outputs. However, in order to reduce the cost of calculations and overcome the hardware and software limitations, it is necessary to adopt some simplification assumptions. A FE model, which was developed in order to predict the creep and superplastic behavior of metal matrix composites in previous studies [12,18,19] is being used here again. The main purpose is to improve the simulation by considering some additional properties. The specifications of the introduced model are as follows.

According to the SEM photos of the cross-section of MMCs [20], it has been seen that the added SiC whiskers to the aluminum matrix are dispersed in the direction of extrusion axis. Also, the photos show that the misalignment of most whiskers is quite small and it can be reasonable to consider them all aligned [21]. Therefore, it could be assumed that the fibers are of circular cross-section and aligned as shown in FIG. 1 (a). Such an assumption makes it possible to simulate the whole composite with an axisymmetric micromechanical model, see FIG. 1 (b). The applied boundary conditions are also presented in FIG. 1 (c).

The fiber/matrix interface debonding is applied to the model according to FIG. 2. Different cases of debonding at the fiber/matrix interface including perfect bond, partial debonding and full debonding are shown in this figure. In fact, fiber/matrix interface debonding is an important parameter in composite deformations, as it has been the case for predicting creep behavior of MMCs [22]. Therefore, this phenomenon is considered in this study, as well. It

should be noted that for the case of creep simulation it was found that $0 \le \zeta \le 0.5$ is meaningful (ζ represents the percentage of the fiber length debonded from the matrix, where for $\zeta = 0.5$ half of a fiber length is considered to be debonded). Above $\zeta = 0.5$, no sign of fiber effects could be distinguished, *i.e*. the matrix creeps as if no fiber presents in the unit. A full explanation of the debonding phenomenon could be found in [18]. Accordingly, $0 \le \zeta \le 0.5$ is considered in this study too. However, it should be noted that the fiber misalignment, fiber offsetting, and the fiber and unit cell geometric ratios (aspect ratios), which could also affect the rate of deformations are ignored here as simplification assumptions.

As for the meshing, uniform nonlinear quadrilateral elements were considered. The Plane-82 of ANSYS element library, which is a 2-D axisymmetric nonlinear elasto-viscoplastic element, is used for the geometry meshing. But, it should be noted that an extraordinary stress filed is developed at the sharp corner of the fiber, where for computing the effects of this field on the inelastic behavior of the material, it is necessary to place very fine mesh in this region [21].

The fiber volume fraction (V_f) is calculated as follows;

(3) $$V_f = \left(\frac{r}{b}\right)^3 \frac{AR_f}{AR_u}$$

where r and b are the fiber and the unit cell radii, and AR_f and AR_u are the fiber and the unit cell aspect ratios, respectively. Here, fiber volume fraction of 20 percent and $AR_f = 4$ are considered.

In this study, it is assumed that the fibers remain elastic during the whole process, while the matrix behaves in an elastic-perfectly plastic manner. Also, a bilinear stress-strain curve with plastic modulus or secant modulus of some value is assumed for the matrix to understand the unusual form of strain vs. cycle diagrams in larger external stresses [19]. A summary of the properties considered for the fiber and the matrix is presented in TAB 1.

TAB 1. Material properties for $\mathrm{Al2024/SiC_W}$ constituents[20]

Material	E [GPa]	CTE [K^{-1}]	ν	σ_y [MPa]
Al 2024	73	24.7×10^{-6}	0.33	30
SiC	470	4.6×10^{-6}	0.17	-

As for the loading, according to the literature available on the experimental superplasticity [20], it is assumed that a thermal cycling regime, as in FIG. 3, along with a small constant tensile mechanical stress is applied to the model. For the heating phase of the cycle, the composite is heated between $100^\circ C - 450^\circ C$ in only 50 seconds, while in cooling half-cycle it is cooled down to $100^\circ C$ from the maximum of $450^\circ C$ during 150 seconds. This thermal cycle is accompanied with a constant longitudinal small mechanical stress of magnitude 2, 4, 7, and 10 MPa [20] to form the biased stress for promoting superplastic deformation.

4. RESULTS AND DISCUSSION

As described before, for the ISS mechanism, the plastic strain starts to accumulate with increasing the number of applied thermal cycles in presence of the mechanical load. It is necessary to introduce the methods of obtaining the results from the FE simulation. One can find the relationship between the strain rate and the corresponding stress according to Backoften's equation [8];

(4) $\sigma = B\dot{\varepsilon}^m$ or $\dot{\varepsilon} = A\sigma^n$ where $m = 1/n$

On the results published in [12], considering the linear relationship of the accumulated plastic strain ($\bar{\varepsilon}_p$) with the number of cycles (N) for all the constant mechanical load cases considered in that study, the strain rate ($\dot{\varepsilon}$) could be obtained from Equation (5);

(5) $$\dot{\varepsilon} = \frac{d\bar{\varepsilon}_p}{dN}.\frac{1}{\tau}$$

where $d\bar{\varepsilon}_p$ represents the accumulated plastic strain in a given number of cycles (*i.e.* dN) and τ indicates the period of the applied thermal cycle [20]. Then the log-log scale plot of the $\dot{\varepsilon}$ values vs. the applied mechanical load indicated a power law type relationship (as in Equation (4)) for the material behavior. There, the power $n = 1.8$ was found to be in a good agreement with the experimental results of $n = 1.6$. Although, some differences between the calculated and the experimentally measured values of $\dot{\varepsilon}$ were evident.

These valuable results were, however, not valid for every point of the model due to the shortcomings of the data collection procedure used in that study. The data was taken from a node inside the matrix close to the interface region in the neighborhood of the fiber end. Replacing the node with another which placed, for example, at the model end, some great differences in the nature and the values of the strain could be realized. In fact, the results of only some

regions of the matrix were in agreement with available experimental data. Therefore, the need for a general data collection was clear and also necessary to develop. This task is fulfilled in the next published paper [19] with the use of averaging idea put forward by Hsueh in [23] for calculation of the average elastic strain, but with applying some modifications to the proposed procedure. In [23], the average values of the nodal and then elemental displacements were used to calculate the average elastic strain. However, since the average plastic strain calculation for the FE modeling is of interest, the average of elemental plastic strain was incorporated into the Equation (6);

$$\bar{\varepsilon}_p = \frac{1}{\pi b^2 L}\sum_{i=1}^{n}\left[\int_{z_{1i}}^{z_{2i}}\int_{r_{1i}}^{r_{2i}} 2\pi\bar{\varepsilon}_{p_i} r\,dr\,dz\right] \quad (6)$$

where $\bar{\varepsilon}_p$ represents the average plastic strain over the entire model, z_i and r_i represent the $z-$ and $r-$ dimensions of the $i\,th$ element, $\bar{\varepsilon}_{p_i}$ is the elemental plastic strain, and b and L are the radius and the length of the model, respectively.

FIG. 4 (a) presents the plastic strain vs. the number of cycles (time) for four mechanical loads of 2, 4, 7, and 10 MPa applied to the model. Interestingly, the results confirm the linear relationship of the $\bar{\varepsilon}_p$ vs. time graphs for all applied stresses, which is the fundamental issue for calculating $\dot{\varepsilon}$ values by the use of Equation (5). To obtain the stress power n in Backoften's equation we should plot the logarithmic diagrams of the calculated $\dot{\varepsilon}$ values vs. the corresponding stresses. Then from the slop of the lines of $\log(\dot{\varepsilon})$ vs. $\log(\sigma)$, one would calculate strain rate sensitivity exponent. Such diagrams are shown in FIG. 5 (a), (b) and (c).

As shown in FIG. 5 (a), the value of n is equal to 1.6 from experimental data, while it drops to 0.6 for the case of the FE simulation with a perfect bond model. To see how the model behaves in presence of fiber/matrix debonding, finite element analysis of the model with $\zeta = 0.125$, 0.25, 0.375 and 0.5 is considered here. As it is seen in FIG. 5 (b), the power n is found to be 1.0 for the model with 12.5% debonding and it is now a little closer to the experimental data. By using a debonding value of 25%, the power n is shifted to 1.8 (FIG. 5 (c)) and the values of $\dot{\varepsilon}$ are also getting closer to the experimental results compared to the case of perfect bond modeling. If we increase the percentages of debonding to reach $\zeta = 0.375$, the values of strain rates are again higher than the results obtained while using a model with $\zeta = 0.25$. But the problem occurs in case of very small mechanical stresses like 2 MPa in which the model behaves as if no fiber presents in the unit and consequently no significant superplastic elongation can be found in the composite. For the case of $\zeta = 0.5$ or 50% debonding, the conditions are even worse and the problem exists for mechanical stresses smaller than 7 MPa.

Another interesting result obtained from the model that could promote further enthusiasm to be put into the efforts for further improvement of the model is related to the little bent or a small change in the slope of the average line of the graph of $\bar{\varepsilon}_p$ vs. time in the middle of the superplastic process for the case of higher values of stresses such as $\sigma = 10$ MPa reported in [12], see FIG. 6. Note the straight line for the case of $\sigma = 2$ MPa. Therefore, it could be concluded that during the superplastic forming of composites, for higher stress values, another mechanism rather than Newtonian viscous flow may come into effect which may need a special treatment. This may cause some problems in manufacturing of MMCs.

This is given a try by considering some deviation in the assumption of elastic-perfectly plastic behavior for the matrix material [19]. This is considered because during the plastic deformation a kind of strain hardening or softening due to the material imperfections or impurities may happen that causes the plastic deformation to go out of the regular expected path. FIG. 7 shows the plastic strain vs. time for $\sigma = 4$ MPa for the case of some percentages of secant modulus that may brought about some small amounts of material strain hardening. As it is seen, in this condition even for small values of applied mechanical stress, a change in slope of the average line of the graph of $\bar{\varepsilon}_p$ vs. time could be detected. However, the decay in the amplitude of the plastic deformation is obvious which is also seen in the same diagrams for higher stress values. Note that the net plastic strain in heating phase of one cycle is negative due to compressive stresses in matrix and conversely, with cooling the composite, the compressive stress disappears and a tensile stress shows up which is resulting in a positive net strain in cooling half-cycle. Remember that the matrix was assumed to be elastic-perfectly plastic.

To investigate the change in superplastic behavior of the composite with respect to the loading profile, another pattern of mechanical stresses is applied here. A combination of various stresses including 8 and 10 MPa is applied to the model during the 40-cycle thermal loading instead of a sole stress of 10 MPa. The resulted diagram of average plastic strain vs. time is shown in FIG. 8. As it is obvious in the diagram, the final values of average plastic strain for both profiles are close to each other although the

sum of the applied stresses is lower for 10-8-10 MPa stress profile. It is interesting to mention that the linearity of the curve can be maintained better by applying a combination of lower stresses. More modeling is under way to find the basic reasons behind the phenomenon and the ways for avoiding the change in the slope.

5. CONCLUSION

From the study performed here one can highlight the followings:

1) The finite element simulation introduced in this study includes an axisymmetric micromechanical model which can predict the behavior of superplastic phenomenon in metal matrix composites although it needs some more modifications before it could be successfully used to analyze all aspects of the superplastic behavior of MMCs.

2) One of the necessary modifications of the model is considering the debonding at fiber/matrix interface. Considering a proper value of debonding for the model can cause the FE results to be closer to the available experimental data.

3) According to the study presented in this paper, the value of the debonding parameter must be chosen between 0 and 0.5 ($0 \le \zeta \le 0.5$). As shown, for $\zeta \ge 0.375$ the modeling can not model the superplastic behavior of the material in small stresses anymore. This study proposed the value of ζ to be considered between 0.125 and 0.25 for similar simulations.

4) It is now clear that there should be a kind of close control over the mechanical loading regime in superplastic forming of materials. At higher loads some sort of strain hardening due to the matrix properties or some kind of softening due to material imperfections may happen that affect the forming process by inflicting necking in the material.

5) By changing the superplastic loading profile properly, manufacturers may be able to achieve better results in superplastic forming. More modeling is necessary to confirm this claim.

6) Further attempts should be made to improve the ability of the introduced model to predict the superplastic behavior of metal matrix composites.

6. FIGURES

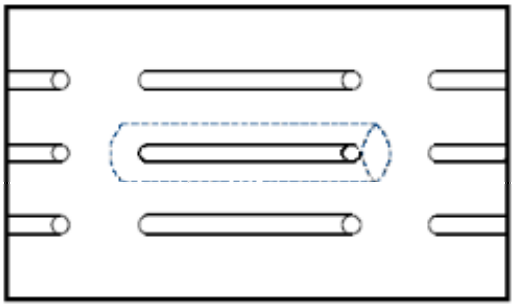

(a)

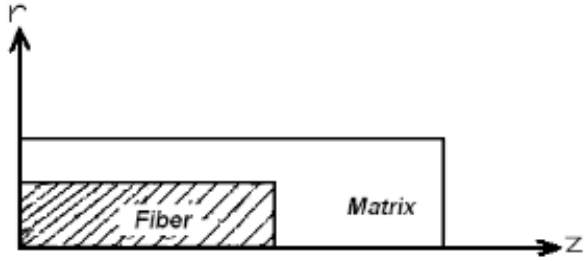

(b)

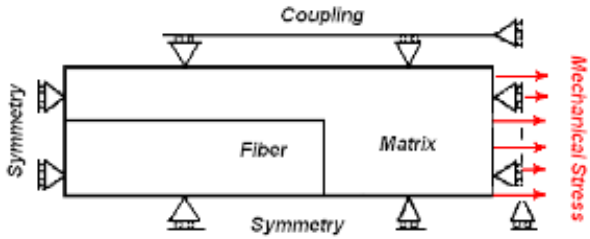

(c)

FIG 1. Geometry modeling of the unit, (a) fiber and matrix in a 3-D model, (b) fiber and matrix in a 2-D model, (c) the final modeling of the fiber and matrix and the boundary conditions

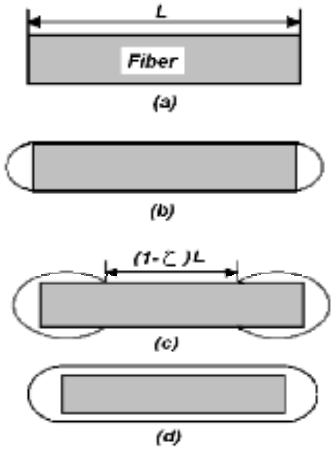

FIG 2. Different situations of debonding at fiber/matrix interface, (a) perfect bond, (b) fiber end debonding, (c) partial debonding, (d) full debonding

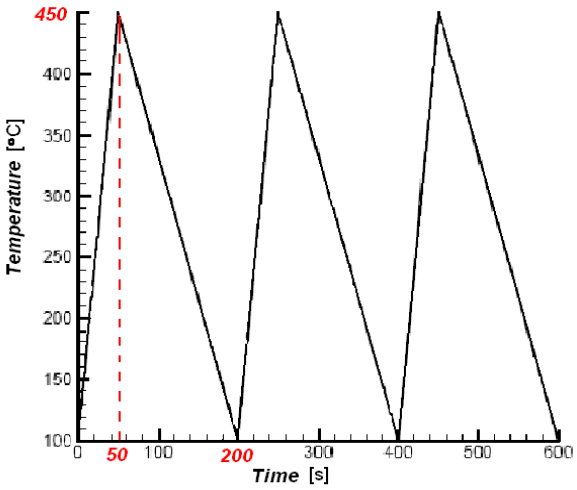

FIG 3. Profile of the applied thermal cycling (only 3 cycles are shown)

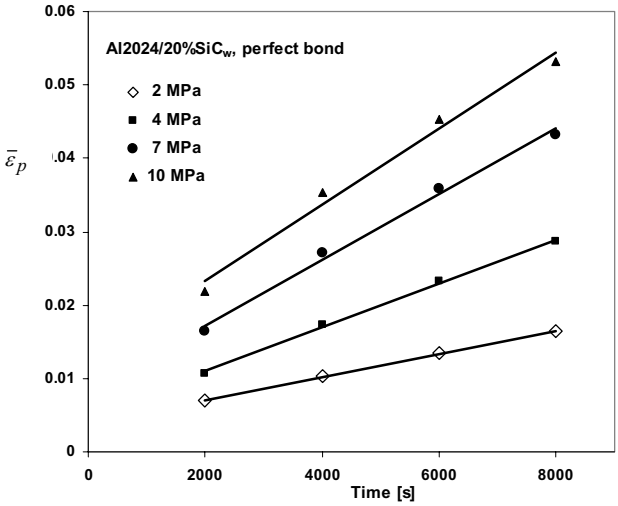

FIG 4. FEM average plastic strain vs. time diagram for Al2024/20%SiC_w (perfect bond) with different applied stress values

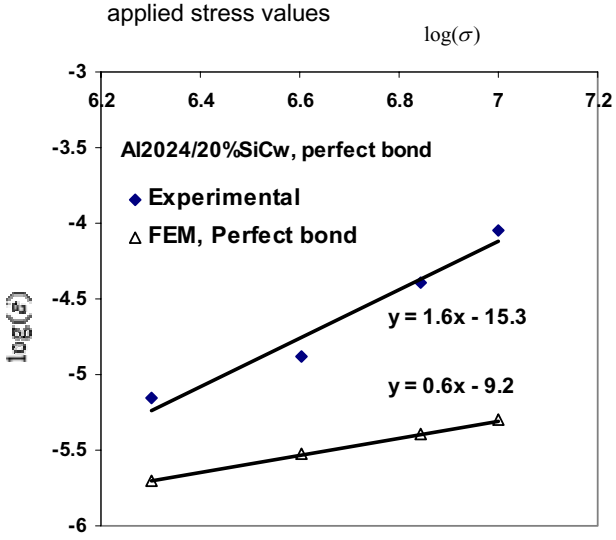

(a)

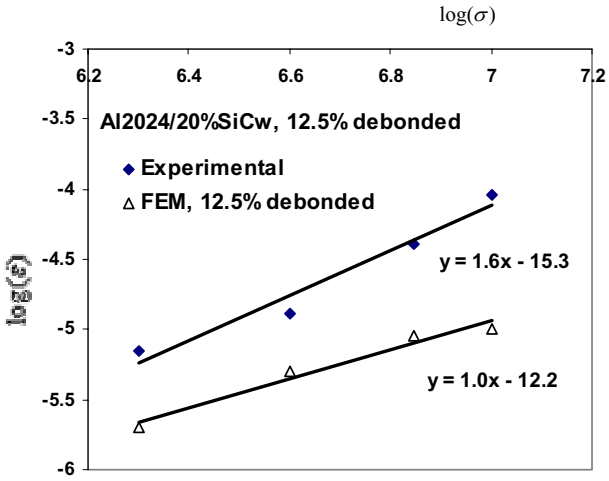

(b)

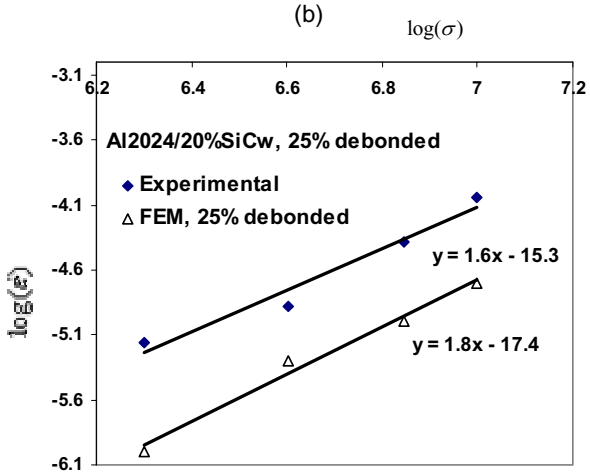

(c)

FIG 5. logarithmic diagram of $\dot{\varepsilon}$ vs. σ for Al2024/20%SiC_w simulation with (a) perfect bond (b) 12.5% debonding (c) 25% debonding

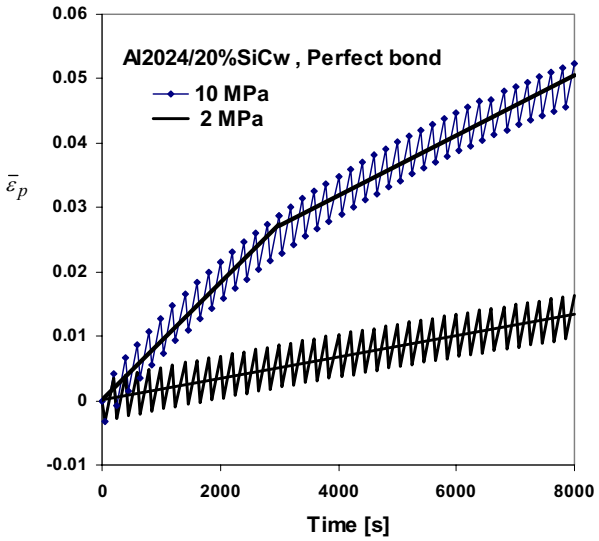

FIG 6. FEM average plastic strain vs. time, showing the change in the slope of the average line for higher stress values

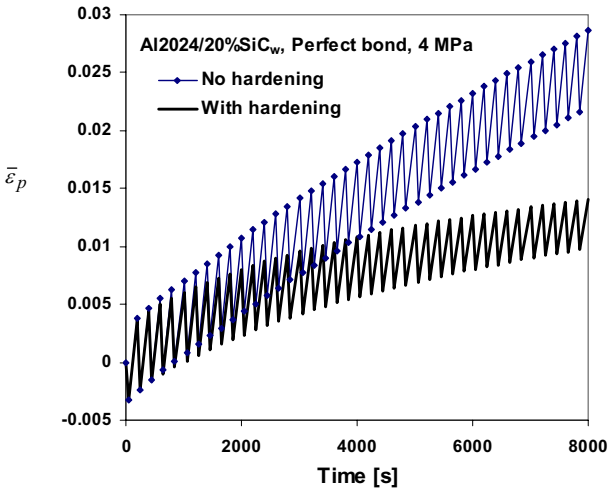

FIG 7. FEM average plastic strain vs. time, considering some values of strain hardening for the matrix material for $\sigma = 4$ MPa

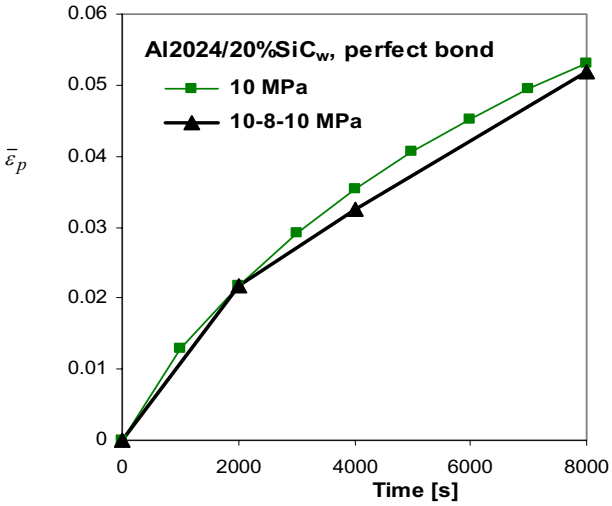

FIG 8. FEM average plastic strain vs. time for two different superplastic loading profile

7. REFERENCES

[1] Chan K.C. and Han B.Q., High-Strain-Rate Superplasticity of Particulate Reinforced Aluminum Matrix Composites, *Int. J. Mech. Sci.*, Vol. 40, pp. 305-311, 1998.

[2] Nieh T.G., Henshall C.A. and Wadsworth J., Superplasticity at high strain rates in a SiC whisker reinforced A1 alloy, *Scripta Metallurgica,* Vol. 18, 1984.

[3] Mabuchi M. and Imai T., Superplasticity of Si3N4 whisker reinforced 6061 aluminum at high strain rate, *Journal of Materials Science Letters,* Vol. 9, 1990.

[4] Sosa S. and Langdon T., Deformation Characteristics of a 3Y-TZP/20%Al2O3 Composite in Tensile Creep, *Material Science Forum*, Vols. 357-359, pp. 135-140, 2001.

[5] Han J., Kim M., Joeng H. and Yamagata H., High Strain Rate Superplasticity in Al-16Si-5Fe Based Alloys with and without SiC Particles, *Material Forum*, Vols. 357-359, pp. 613-618, 2001.

[6] Sherby O., Advances in Superplasticity and in Superplastic Materials, *ISIJ International*, Vol. 29, 1989.

[7] Sunder R., Kitazono K., Sato E. and Kuribayashi K., Internal Stress Superplasticity in an in-situ Intermetallic Matrix Composite, *Materials Science Forum*, Orlando, USA, pp. 405-410, 2001.

[8] Xing H., Wang C., Zhang K. and Wang Z., Recent Development in the Mechanics of Superplasticity & its Applications, *J. of Materials Processing Technology*, pp. 196-202, 2004.

[9] Nieh T., Wadsworth J. and Sherby O., *Superplasticity in Metals and Ceramics*, Cambridge University Press, 1997.

[10] Pickard S. and Derby B., The Deformation of Particle Reinforced Metal Matrix Composites during Temperature Cycling, *Acta Metal. Mater.*, Vol. 38, No. 12, pp. 2537-2552, 1990.

[11] Derby B., Internal Stress Superplasticity in Metal Matrix Composites, *Scripta Metall.*, Vol. 19, pp. 703, 1985.

[12] Abedian A. and Malekpour A., FEM Analysis of Internal Stress Superplasticity in Al/SiC_w Composite with Different V_F Subjected to Thermal Cycling, 24th ICAS, 2004.

[13] Mimaroglu A. and Yeinhayat O., Modeling the Superplastic Deformation Process of 2024 Aluminum Alloys under Constant Strain Rate: Use of Finite Element Technique, *Material and Design*, pp. 189-195, 2003.

[14] Zhang H., Daehn G. and Wagoner R., Simulation of Plastic Response of Whisker Reinforced Metal Matrix Composites under Thermal Cycling Conditions, *Scripta. Metal. Mater.*, Vol. 25, pp. 2285-2290, 1991.

[15] Zwigl and Dunand D., Transformation-mismatch Plasticity of NiAl/ZrO_2 Composites: Finite Element Modeling, *Materials Science & Engineering A.*, 2002.

[16] Carrino, Giuliano and Palmieri, On the Optimization of Superplastic Forming Processes by the Finite Element Method, *Materials Processing Technology*, pp. 373-377, 2003.

[17] Yarlagadda, Gudimetla and Adam, Finite Element Analysis of High Strain Rate Superplastic Forming (SPF) of Al-Ti Alloys, *Material Processing Technology*, 2002.

[18] Mondali M., Abedian A. and Adibnazari A., FEM Study of the Second Stage Creep Behavior of Al6061/SiC Metal Matrix Composite, *Computational Material Science*, pp. 140-150, 2005.

[19] Abedian A., Barakati A. and Malekpour A., Effects of Geometry Aspects on the Simulation of Superplasticity in MMC Composites, 25th ICAS, 2006.

[20] Hong S., Sherby O., Divecha A., Karmarker S. and McDonald B., Internal Stress Superplasticity in 2024Al-SiC Whisker Reinforced Composites, *Journal of Composite Materials*, Vol. 22, pp. 102-123, 1988.

[21] Chan K. and Tong G., Strain Rate Sensitivity of a High-strain-rate Superplastic Al606/SiCw Composite under Uniaxial and Equibiaxial Tension, *Materials Letters 51*, 2001.

[22] Abedian A. and Mondali M., FEM Study of Constant Rate Creep Analysis of MMCs, 11th Iranian Annual Conference (International) of Mechanical Engineering, Vol. 3, pp. 1271-1280, 2003.

[23] Hsueh Chaun-Hway, Young's Modulus of Unidirectional Discontinuous-fiber Composites, *Composites Science and Technology*, pp. 2671-2680, 2000.